Available online at www.eccomasproceedia.org
Eccomas Proceedia COMPDYN (2023) 3994-4003

ECCOMAS
Proceedia

COMPDYN 2023
9th ECCOMAS Thematic Conference on
Computational Methods in Structural Dynamics and Earthquake Engineering
M. Papadrakakis, M. Fragiadakis (eds.)
Athens, Greece, 12-14 June 2023

VERIFICATION OF MATERIAL MODELS FOR MASONRY WALLS IN NONLINEAR PUSHOVER ANALYSIS

H. He[1] and S. J. H. Meijers [2]

[1 2]Advanced Technology and Research, Industry & Buildings, HaskoningDHV Nederland B.V., Rotterdam, the Netherlands
[1]e-mail: huan.he@rhdhv.com; [2]e-mail: sander.meijers@rhdhv.com

Abstract

Masonry material model used in the non-linear pushover (NLPO) analysis plays an important role for the building responses. Different material models based on the smeared failures for unreinforced masonry (URM) wall are tested and compared in the in-plane nonlinear pushover analysis in this study. Special attentions are paid on the base shear versus displacement curves and the failure modes (crack pattern) in the analysis. Influences by the geometric shape ratio (i.e. height/width), the overburden level, boundary conditions and masonry type are discussed in the paper. Meanwhile, numerical results of selected URM walls with different material models are compared to the analytical ones based on the codes. Eventually, the most suitable material model for masonry walls in NLPO analysis is identified in the paper.

Keywords: Unreinforced masonry walls, Nonlinear pushover analysis, Engineering masonry model, FEM.

ISSN:2623-3347
Peer-review under responsibility of the organizing committee of COMPDYN 2023.
doi: 10.7712/120123.10697.20791

1 INTRODUCTION

The seismic risk in Groningen area of the Netherlands is induced by the gas extraction. The frequency of the shallow earthquakes is generally increased year by year (over 80 times per year in the recent decade), which received a great concern by the Dutch society. Therefore, a framework for the seismic assessment and retrofitting design of structures in the Groningen region, called VIIA, was initiated and developed from 2015. Different approaches have been used for the purpose of seismic analysis, *e.g.* modal response spectrum (MRS) analysis, non-linear pushover (NLPO) analysis, nonlinear time-history (NLTH) analysis and reference approach, *etc*.

NLPO analysis is a simple static seismic technique, which is therefore commonly used for the evaluations of existing buildings. In the NLPO analysis, the determination of a global base shear versus displacement curve (called the pushover curve) is fundamental for the assessment. Meanwhile, unreinforced masonry (URM) wall is one of the most vulnerable structural elements for the buildings in the area. The selection of material models of masonries can directly influence the performances of buildings in NLPO analysis. Therefore, it is crucial to identify the performances of different material models for masonry in the NLPO analysis using a FEA software, *i.e.* DIANA[1].

The global behavior of building in NLPO analysis is largely influenced by the in-plane response of individual components in the structure system such as the piers and spandrels. Accordingly, in-plane pushover tests on single unreinforced masonry (URM) walls with different material models are performed in DIANA software in the study. The base shear versus displacement curves and the failure modes (crack pattern) will be focused in the analysis. For URM walls, the maximum shear capacity and the expected failure modes are influenced by the geometric shape ratio (height/width, H/L), the overburden level, boundary conditions and masonry types. It can also be estimated based on formulas from codes, e.g. NPR 9998:2017[2], Eurocode 6[3]. Therefore, selected URM walls with different material model are tested in NLPO analysis and the results are compared to the analytical ones. The most suitable material model for masonry walls in NLPO analysis is, therefore, identified.

2 MASONRY MATERIAL MODEL

Masonry is one of the oldest but still popular construction materials. Its properties largely depend on the components and the arrangement. Generally, there are two modelling methods used for the simulation of masonry, *i.e.* micro-modelling and macro-modelling[4]. Every component of masonry is separately modelled by the micro-modelling method. Therefore, the crack propagation and failure mechanism can be realistically simulated detailly by this method. However, this method is not feasible for the structural assessment of large masonry buildings due to the computational consumption. Therefore, macro-modelling method is a good alternative. It considers masonry as a composite material. Generally, continuum and homogeneous properties are assumed for the masonry by this method.

Total Strain Crack Model (TSCM) is one of the continuum constitutive models, which can be used for the simulation of masonry. It follows a smear approach for the fracture energy[1]. Regarding its evaluation of stress-strain relationship, one method is following the principal direction of strain vector, which is called the rotating crack model (TSCM-rotating). Another method is using the fixed coordination system, which is called the fixed crack model (TSCM-fixed) [1]. Both of these two approaches use a secant-based loading-unloading curve. Therefore, it underestimates the energy dissipation of masonry under the cyclic loading compared to the experimental references[5]. Meanwhile, TSCM is developed for the isotropic materials, which is not the case for masonry.

Therefore, a comprehensive masonry material model *i.e.* Engineering Masonry Model (EMM) has been developed in DIANA, which can consider the orthotropic mechanical properties (in tension, compression and shear) and hysteresis damping effects[5]. The new developed model has been verified by the comparison with quasi-static experimental references both under in-plane and out-of-plane (OOP) loadings[5]. One example comparison was done with a OOP pushover test[6,7], shown in Figure 1. Moreover, a comparison study has been done with the dynamic one-way out-of-plane shaking table tests[8], which validated the EMM parameters.

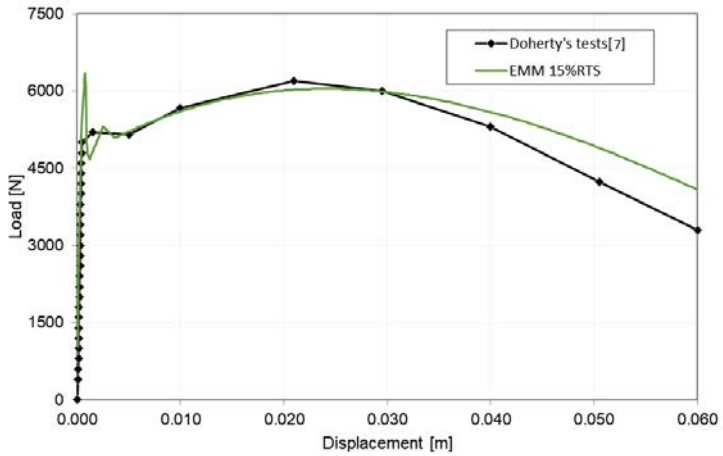

Figure 1: Static pushover comparison under OOP loading[6]

3 TESTING MODELS

The material models tested in this report are the Engineering Masonry Model (EMM) and the two Total Strain-based Crack Models, *i.e.* TSCM-rotating and TSCM-fixed. For the application of the incremental load, a simple top (whole edge tied) horizontal displacement-controlled pushover method is used in the test. There are two vertical constrain conditions for the top edge: free and entirely fixed, which will be discussed separately later in the study. The masonry walls are all 2.76 m high and 0.102 m thick, but with different width (the different shape ratio H/Ls, see Figure 2). Three types of Groningen masonries made by clay bricks, defined in NPR 9998:2017[2], *i.e.* normal clay brickwork pre 1945 (BKv), poor clay brickwork pre 1945 (BKvl) and clay brickwork post 1945 (BKn), are used in the tests (listed Table 1). Other materials parameters of masonries can be referred by Table F2 of NPR 9998:2017[2]

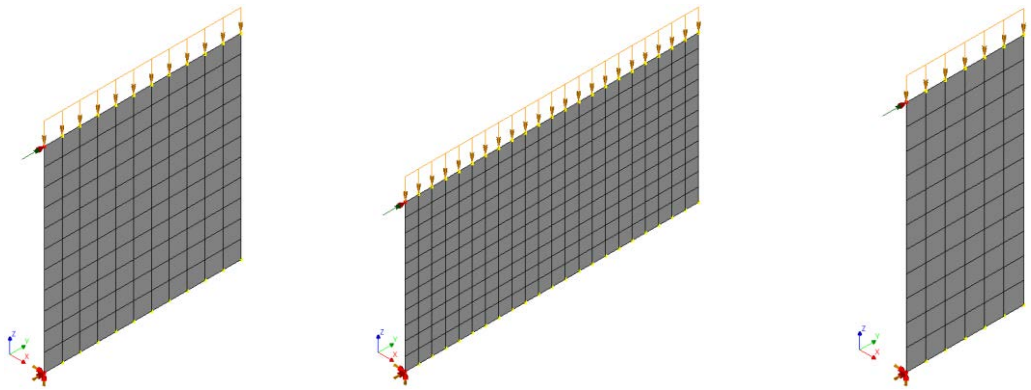

(a) (b) (c)

Figure 2: Three models used in the study with different shape ratios: (a)H/L=1; (b) H/L=1:2; (c) H/L=2:1

Masonry	f_c (N/m^2)	L (m)	H/L (-)	R_OB1 (-)	OB1 force (N/m)	R_OB2 (-)	OB2 force (N/m)	Visualization
BKv	8.50E+06	2.76	1	0.2	1.73E+05	0.02	1.73E+04	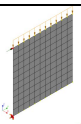
BKvl	5.10E+06	2.76	1	0.2	1.04E+05	0.02	1.04E+04	
BKn	1.00E+07	2.76	1	0.2	2.04E+05	0.02	2.04E+04	
BKv	8.50E+06	5.52	0.5	0.2	1.73E+05	0.02	1.73E+04	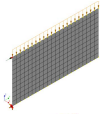
BKvl	5.10E+06	5.52	0.5	0.2	1.04E+05	0.02	1.04E+04	
BKn	1.00E+07	5.52	0.5	0.2	2.04E+05	0.02	2.04E+04	
BKv	8.50E+06	1.38	2	0.2	1.73E+05	0.02	1.73E+04	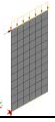
BKvl	5.10E+06	1.38	2	0.2	1.04E+05	0.02	1.04E+04	
BKn	1.00E+07	1.38	2	0.2	2.04E+05	0.02	2.04E+04	

Note: f_c: compressive strength of masonry; OB: overburden load; R_OB: ratio of overburden load to the compressive strength of the masonry, P_{OB}/f_c;

Table 1: Specifications of tested models.

4 ANALYTICAL ESTIMATION

NPR9998:2017[2] specifies different failure mechanisms and the corresponding shear capacities. Diagonal tensile capacity failure occurs when the principal stress is exceeding diagonal tensile strength. Toe crushing failure should also be considered for the shear loading. Rocking failure occurs commonly when wall is slender and mortar strength is relatively good. Bed-joint sliding is a stable mode of failure, which should be considered in the evaluation. Different capacities due to different mechanisms are specified in Table 2 following NPR 9998:2017[2]. Moreover, Eurocode 6 specifies shear capacities of walls with similar but simpler formulas[3].

Failure mechanism	*Capacity* formula	Explanation
Diagonal tensile capacity (DTC) V_{dt}	$V_{dt} = f_{dt} \times A_n \times \beta \times \sqrt{1 + \frac{f_a}{f_{dt}}}$ $f_{dt} = 0.5 \times c + f_a \times \mu_f$	β is a nonlinear corrector factor, which is 0.67 if H/L>1.5 and 1.0 if H/L<0.5; A_n is the net area of mortared/grouted section; f_{dt} is the masonry tensile strength; f_a is the axial compressive stress at mid-height; c is the bed-joint cohesion; μ_f is the frictional coefficient; α is a boundary factor, which equals 0.5 for fix-free cantilever and equals 1 for fixed-fixed case; P is the overburden load at top of wall; P_w is the self-weight of wall; t_{norm} is the nominal thickness of masonry brick excluding pointing.
Toe crushing V_{tc}	$V_{tc} = (\alpha \times P + 0.5 \times P_w)(\frac{L}{H})(1 - \frac{f_a}{f_c})$	
Rocking strength V_r	$V_r = 0.9 \times [(\alpha \times P) + (0.5 \times P_w)] \times (\frac{L}{H})$	
Bed-joint sliding (BJS) V_s	$V_s = 0.7 \times [t_{norm} \times L \times c + \mu_f (P + P_w)]$	

Table 2: Different capacity formulas based on the failure mechanisms in NPR9998:2017[2].

5 RESULTS AND DISCUSSION

Based on the above specifications, different wall models are tested in in-plane NLPO analysis by DIANA. Only some selected results are presented in the paper due to the space limitation. The pushover curves and corresponding crack patterns at the peak force with different material models are shown for the different cases. Figure 3 and Figure 4 are for the case with H/L=1.0, BKv material, overburden OB1 and the fixed-free boundary condition. Figure 5 and Figure 6 are for the case with H/L=1.0, BKv material, overburden OB2 and the fixed-free boundary condition. Figure 7 and Figure 8 are for the case with H/L=0.5, BKv material, overburden OB1 and the fixed-free boundary condition. Figure 9 and Figure 10 are for the case with H/L=2.0, BKv material, overburden OB1 and the fixed-free boundary condition. Figure 11 and Figure 12 are for the case with H/L=1.0, BKv material, overburden OB1 and the fixed-fixed boundary condition.

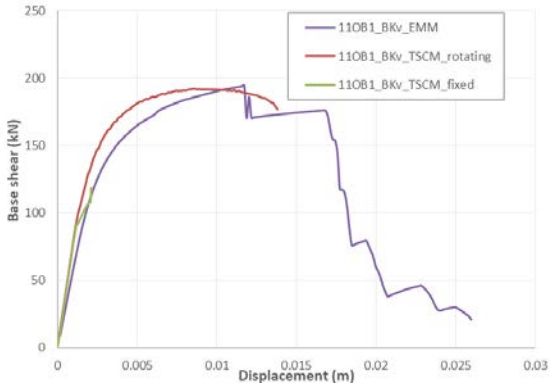

Figure 3: Base shear-displacement curves for walls with H/L=1.0, BKv material, overburden OB1, fixed-free boundary condition and different material models

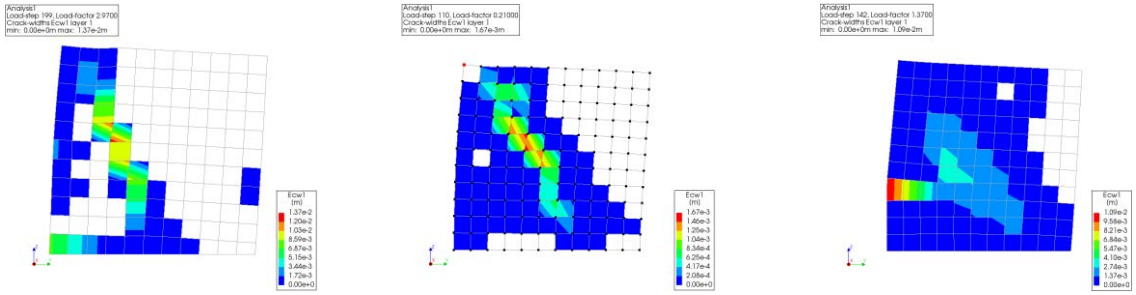

(a) (b) (c)

Figure 4: Crack width patterns of masonry walls at the peak force with condition of Figure 3: (a) EMM; (b)TSCM-fixed; (c)TSCM-rotating.

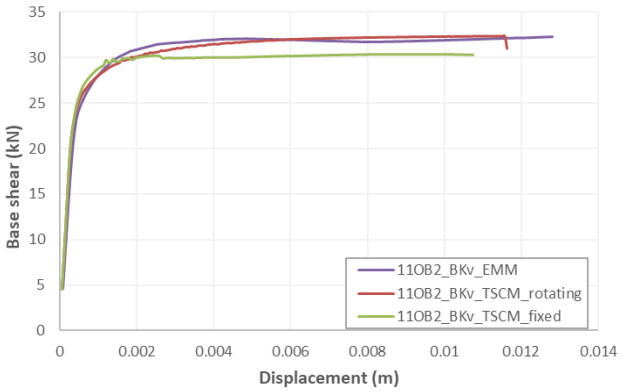

Figure 5: Base shear-displacement curves for walls with H/L=1.0, BKv material, overburden OB2, fixed-free boundary condition and different material models

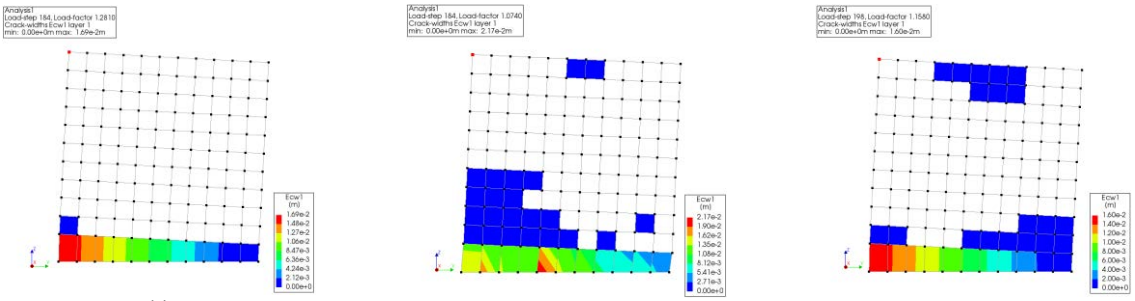

(a) (b) (c)

Figure 6: Crack width patterns of masonry walls at the peak force with condition of Figure 5: (a) EMM; (b)TSCM-fixed; (c)TSCM-rotating.

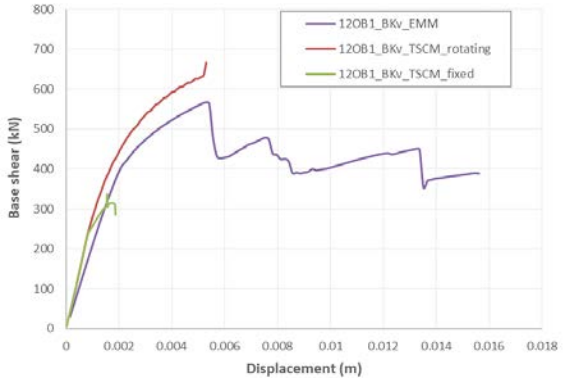

Figure 7: Base shear-displacement curves for walls with H/L=0.5, BKv material, overburden OB1, fixed-free boundary condition and different material models

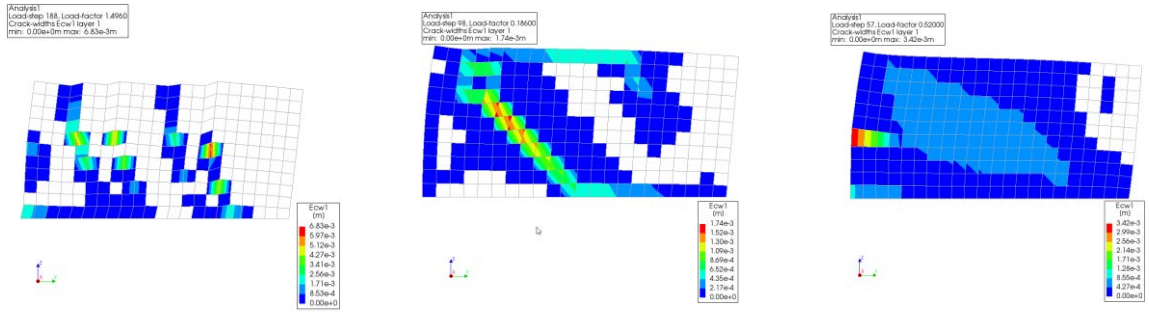

(a) (b) (c)

Figure 8 Crack width patterns of masonry walls at the peak force with condition of Figure 7: (a) EMM; (b)TSCM-fixed; (c)TSCM-rotating.

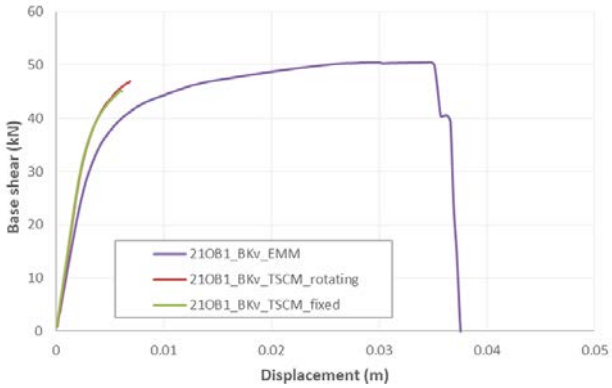

Figure 9: Base shear-displacement curves for walls with H/L=2, BKv material, overburden OB1, fixed-free boundary condition and different material models

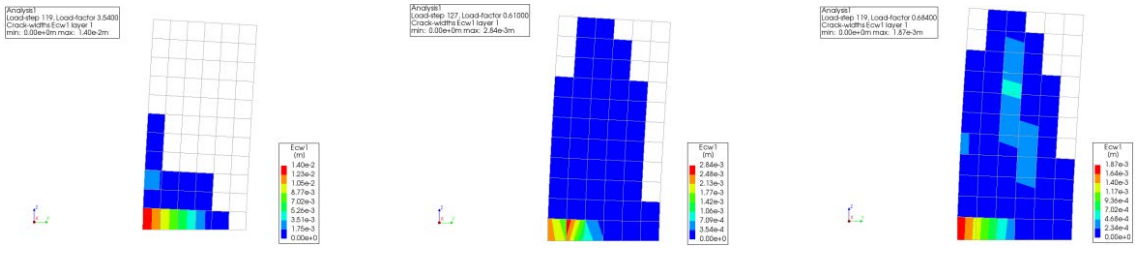

(a) (b) (c)

Figure 10: Crack width patterns of masonry walls at the peak force with condition of Figure 9: (a) EMM; (b)TSCM-fixed; (c)TSCM-rotating.

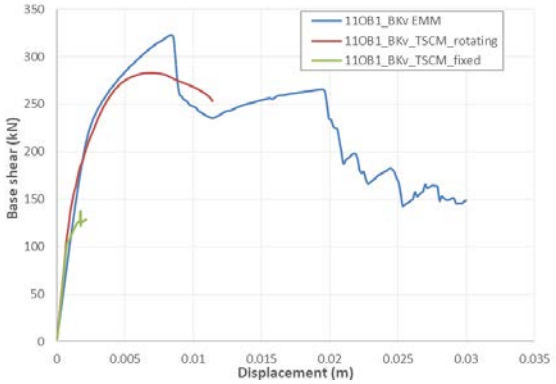

Figure 11: Base shear-displacement curves for walls with H/L=1, BKv material, overburden OB1, fixed-fixed boundary condition and different material models

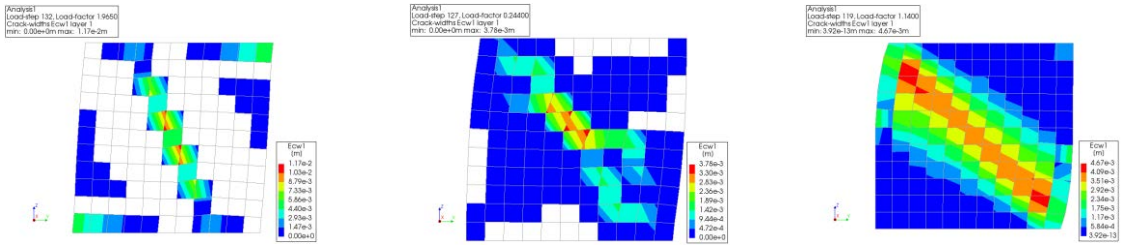

(a) (b) (c)

Figure 12: Crack width patterns of masonry walls at the peak force with condition of Figure 11: (a) EMM; (b)TSCM-fixed; (c)TSCM-rotating.

Above results show that model with TSCM-rotating has a closer response to the model with EMM compared to the TSCM-fixed. Meanwhile, models with EMM present generally a more stable post-peak behavior, which means that a higher ductility can be observed in push-over curves. This is especially true for cases with a higher overburden load. Moreover, models with the vertically free top edges and a lower overburden load are more stable for all material models. Models with a higher overburden and fixed top boundary condition have higher in-plane shear capacities.

Following the methods described in Section 4, shear capacities of masonry walls are estimated based on different failure mechanisms by NPR 9998:2017[2] and Eurocode 6 (EC6) [3], listed in Table 3 and Table 4 for cases with fixed-free and fixed-fixed boundary conditions, respectively. Meanwhile, the capacities with different material models revealed by the numerical results are also listed in the table for the comparison purpose. The results shows that the prediction method based on NPR 9998: 2017[1] provides more detailed information based on the different mechanisms than one based on the Eurocode 6[3]. In general, the results by NPR 9998:2017 correlate well with the numerical results obtained in this study, especially those with EMM and TSCM-rotating.

H/L	P_{OB}/f_c (-)	Masonry	EC6[3] moment based (kN)	EC6[3] shear based (kN)	NPR[2] DTC (kN)	NPR[2] toe crush (kN)	NPR[2] rocking (kN)	NPR[2] BJS (kN)	NPR[2] Min. (kN)	EMM peak (kN)	TSCM-fixed peak (kN)	TSCM-rotating peak (kN)
1	0.2	BKv	190.8	370.4	503.3	175.2	222.2	318.4	175.2	195	118	192
		BKvl	130.1	136.1	211.0	106.9	136.1	121.5	106.9	89	77	116
		BKn	212.1	433.7	596.8	205.4	260.2	382.4	205.4	224	180	228

H/L	P_{OB}/f_c (-)	Masonry	EC6[3] moment based (kN)	EC6[3] shear based (kN)	NPR[2] DTC (kN)	NPR[2] toe crush (kN)	NPR[2] rocking (kN)	NPR[2] BJS (kN)	NPR[2] Min. (kN)	EMM peak (kN)	TSCM-fixed peak (kN)	TSCM-rotating peak (kN)
0.5	0.02	BKv	30.6	47.3	90.2	22.4	28.4	92.2	22.4	32	30	32
		BKvl	21.5	33.0	46.2	15.5	19.8	48.0	15.5	22	21	22
		BKn	34.6	53.7	110.6	25.4	32.2	116.4	25.4	38	37	38
	0.2	BKv	269.2	740.7	1205.6	701.0	888.9	636.8	636.8	566	337	635
		BKvl	218.2	272.2	505.4	427.4	544.3	243.0	243.0	229	198	371
		BKn	270.3	867.4	1429.6	821.6	1040.9	764.9	764.9	680	462	775
2	0.02	BKv	59.4	94.7	216.2	89.6	113.6	184.5	89.6	123	83	84
		BKvl	42.2	65.9	110.7	62.1	79.1	96.0	62.1	73	50	64
		BKn	66.8	107.3	264.8	101.7	128.8	232.8	101.7	144	120	143
	0.2	BKv	109.4	185.2	201.9	43.8	55.6	159.2	43.8	51	45	47
		BKvl	70.3	68.0	84.7	26.7	34.0	60.8	26.7	30	27	27
		BKn	125.3	216.9	239.5	51.4	65.1	191.2	51.4	60	59	59
	0.02	BKv	15.5	23.7	36.2	5.6	7.1	46.1	5.6	9	8	8
		BKvl	10.9	16.5	18.5	3.9	4.9	24.0	3.9	6	5	6
		BKn	17.6	26.8	44.4	6.4	8.0	58.2	6.4	10	10	10

Table 3: Peak base shears of different models and the corresponding analytical predictions[7,8], with the fixed-free boundary condition.

H/L	P_{OB}/f_c (-)	Masonry	EC6[3] moment based (kN)	EC6[3] shear based (kN)	NPR[2] Tensile-diagonal (kN)	NPR[2] toe crush (kN)	NPR[2] rocking (kN)	NPR[2] BJS (kN)	NPR[2] Min. (kN)	EMM peak (kN)	TSCM-fixed peak (kN)	TSCM-rotating peak (kN)
1	0.2	BKv	190.8	370.4	503.3	345.1	437.6	318.4	318.4	323	138	283
		BKvl	130.1	136.1	211.0	208.3	265.3	121.5	121.5	118	76	171
		BKn	212.1	433.7	596.8	405.4	513.6	382.4	382.4	386	212	337
	0.02	BKv	30.6	47.3	90.2	39.4	49.9	92.2	39.4	59	41	41
		BKvl	21.5	33.0	46.2	25.7	32.7	48.0	25.7	38	25	25
		BKn	34.6	53.7	110.6	45.4	57.5	116.4	45.4	71	60	69
0.5	0.2	BKv	269.2	740.7	1205.6	1380.3	1750.3	636.8	636.8	704	369	845
		BKvl	218.2	272.2	505.4	833.3	1061.2	243.0	243.0	268	204	509
		BKn	270.3	867.4	1429.6	1621.6	2054.4	764.9	764.9	831	464	1001
	0.02	BKv	59.4	94.7	216.2	157.5	199.7	184.5	157.5	157	96	175
		BKvl	42.2	65.9	110.7	102.7	130.8	96.0	96.0	94	59	106
		BKn	66.8	107.3	264.8	181.7	230.1	232.8	181.7	206	152	203
2	0.2	BKv	109.4	185.2	201.9	86.3	109.4	159.2	86.3	107	44	47
		BKvl	70.3	68.0	84.7	52.1	66.3	60.8	52.1	48	26	29
		BKn	125.3	216.9	239.5	101.4	128.4	191.2	101.4	126	71	69
	0.02	BKv	15.5	23.7	36.2	9.8	12.5	46.1	9.8	16	14	17
		BKvl	10.9	16.5	18.5	6.4	8.2	24.0	6.4	10	9.3	10.9
		BKn	17.6	26.8	44.4	11.4	14.4	58.2	11.4	19	19	20

Table 4: Peak base shears of different models and the corresponding analytical predictions[7,8], with the fixed-fixed boundary condition.

6 CONCLUSIONS

In this study, URM walls with different Groningen masonries of clay brickwork are numerically tested by the NLPO method using different material models. The influences of other factors, *e.g.* overburden loads, shape ratio, boundary conditions, etc. are also discussed in the study. Furthermore, numerical results are compared with the theoretical estimations by NPR 9998:2017[2] and Eurocode 6[3]. Based on the in-plane NLPO test results, some conclusions are drawn as follows.

- Compared to the model with TSCM-fixed, model with TSCM-rotating has closer responses to the one with EMM.
- Models with EMM present generally a more stable post-peak behavior, which reveals a higher ductility. This is especially true for cases with a higher overburden load.
- In general, the prediction method based on NPR 9998: 2017[2] provides more detailed information based on the different mechanisms than one based on the Eurocode 6[3]. The results based on NPR 9998:2017 correlate well with the numerical results obtained in this report, especially those with EMM and TSCM-rotating.
- There are a few cases that capacities of models with EMM is higher than the ones based on NPR 9998: 2017[2]. This may be due to the more comprehensive definitions of masonry material by EMM, which could be studied in the future.
- Based on the comparison study, the EMM presents a better behavior than the other options. Hence it is recommended to select this material model as the preferable default masonry model for the NLPO analysis in DIANA for the URM objects.

REFERENCES

[1] DIANA FEA, *Finite Element Analysis*: *release 10.5*, DIANA FEA BV, Delft, the Netherlands, 2020

[2] NEN, *NPR 9998: 2017, Beoordeling van de constructieve veiligheid van een gebouw bij nieuwbouw, verbouw en afkeuren – Grondslagen voor aardbevingsbelastingen: geïnduceerde aardbevingen*, NEN. 2018.

[3] European Committee for Standardization, *Eurocode 6: design of masonry structures—part 1-1: general rules for reinforced and unreinforced masonry structures.* European Committee for Standardization, Brussels, Belgium, 2006

[4] F.J. Noortman, *Applicability of the pushover method for the seismic assessment of URM structures in Groningen: a case study of a low-rise building*, Master thesis, TU Delft, 2019.

[5] G.M.A. Schreppers, A. Garofano, F. Messali, J.G. Rots, *DIANA Validation Report for Engineering Masonry Model*, TNO DIANA report 2016-DIANA-R1601, TU Delft Structural Mechanics CITG report CM-2016-17. 2016.

[6] H. He, *Out-of-plane Performance of EMM: Validation by the Static and Seismic tests*, VIIA report, 2016.

[7] K.T. Doherty, *An investigation of the weak links in the seismic load path of unreinforced masonary buildings*. PhD Thesis, University of Adelaide, Australia. 2000.

[8] H. He, S.J.H. Meijers, R.A. Vonk, F.H. Middelkoop, Numerical study on the seis-mic out-of-plane performance of URM walls, J. Kubica, A. Kwiecień & Ł. Bednarz (Eds),

Proceeding of 17th International Brick and Block Masonry Conference (17IB2MaC), Krakow, Poland in July 5-8, 2020. 916-923, Taylor & Francis Group, 2020.